

Real Time Digital Processing of GPS Measurements for Transmission Engineering

C. Mensah-Bonsu
Student Member, IEEE

G. T. Heydt
Fellow, IEEE

Arizona State University
Tempe, Arizona, USA

Abstract: The Global Positioning System (GPS) is a state of the art timing and positioning system based on 24 or more satellites launched and maintained by the United States government. Power engineering applications based on the GPS include phasor measurement, positioning applications such as surveying and mapping, and potentially in deriving real time data on transmission lines that will allow them to be loaded to a dynamic (thermal or security) limit. Inherent errors in GPS technologies are discussed, and the differential GPS method is described for accuracy enhancement. Further digital processing needs are necessary for meeting the accuracy requirements of certain specific applications. The focus of this paper is on the digital signal processing (DSP) of differential GPS (DGPS) measurements. The paper describes a methodology for further improving DGPS altitude measurements for the purpose of accurate determination of high voltage overhead conductor sag. The wavelet transforms and least squares parameter estimation (LSPE) techniques are considered.

Keywords: GPS; overhead conductor sag; wavelet analysis; least squares parameter estimation; dynamic thermal line rating; transmission engineering.

I. Introduction

The Global Positioning System is a positioning and timing system based on 24 satellites in operation. The satellites were launched and are maintained by the United States government. Each satellite orbits the Earth in approximately 12 hours. Implemented initially with military applications in mind, the GPS/DGPS technology is highly reliable. Various engineering and military applications of the GPS and, its basic technological concepts are described in [3, 4, 6, 18]. The essence of the GPS technology is a receiver clock offset and 3-D position of GPS receivers which are determined from measured satellite-to-receiver ranges called *pseudorange*. The pseudorange is based on four or more GPS satellite signal reception. For certain national security considerations, the GPS technology had originally intentionally inserted error known as SA (Selective Availability). In 2000, the SA error of 0.2 μ s (60 m) was removed [21]. Errors due to the propagation of the signals from GPS satellites, errors in solving the system of pseudorange equations, and other errors occur. The presence of bad GPS measurement data could be attributed to a variety of sources, some of which are not fully understood. The momentary loss of some GPS satellites from view will negatively impact the measurement accuracy. Also, interference and signal

reflections degrade accuracy. In addition, the ambient noise impacts solution accuracy. Other error mechanisms may also create single datum values that are erroneous. One way to reduce these errors involves the comparison of a GPS position calculation with that at a known surveyed position. In this way, an error or a difference is generated which is then used as a correction. The concept is called differential GPS [3] and the technology is further denominated depending on the collection of the final position result at the surveyed base station (*direct DGPS*) or the 'rover' remote station (*inverse DGPS*). More recently there has been recommendations to add an additional frequency to the system. This is intended to improve the accuracy of civilian GPS applications. The DGPS operation offers significant position accuracy improvement over standard GPS. DGPS compensation greatly attenuates errors common to all local receivers in use. However, spatial correlation of atmospheric delays could cause the DGPS position accuracy to deteriorate with increasing distance between the reference and rover receivers. Equation (1) describes the autocorrelation function, $R(d)$ between two points separated by a distance d of correlation distance D and variance σ^2 as [7],

$$R(d) = E(x_1, x_2) = \sigma^2 e^{(-d/D)} \quad (1)$$

where, x_1 and x_2 are the respective pseudorange errors at receiver positions 1 and 2.

The following accounts for the increase use of DGPS: nanosecond-order precise time tagging capability (accuracy), compactness, portability, low cost and, around the clock operation in all weather conditions anywhere on Earth. DGPS has been used for different applications including dispatching/fleet management, emergency tracking, offshore exploration and, agriculture [3].

The main applications of GPS technology in power engineering have been in:

- Surveying
- Mapping
- System protection
- Phasor measurement in real time.

In addition, recently, DGPS has been proposed for the measurement of overhead conductor sag in transmission circuits [1]. In that application, the main concept was the use of a DGPS based instrument to accurately estimate the position of a point on the overhead con-

ductor in a critical transmission line span. The goal was to convert this conductor sag data to a dynamic (real time) thermal rating of the line [1, 2, 8,10, 11, 18]. The main results reported in this paper were obtained in prototyping the overhead conductor sag instrument. The utilization of GPS technology for phasor measurements and surveying in power engineering is well known: and these technologies do not have problems in accurate measurements of time and horizontal (i.e., $x - y$) position. The measurement of vertical position (i.e., z), however, is more problematic because some compromises were made in the GPS design to attain accuracy in $x - y$ measurements. For this reason, the remaining focus of this paper relates to the digital signal processing of vertical DGPS measurement for transmission engineering applications.

II. Digital processing of GPS data

The GPS technology is heavily based on DSP. The pseudorandom signals from the GPS system are digitally decoded, converted to pseudorange data, and solved for position and time at the receiver – all digitally. Evidence about the error in raw GPS measurement data has been reported since the inception of the technology over two decades ago. The measurement errors can be traced to various sources including multipath, ionospheric, tropospheric effects and, clock offset [3, 4]. A distribution of errors that affect the x , y and z positioning accuracy due to specifically selected factors are given in Table 1.

Table 1. Error distribution in meters [3, 4]

| Error source | GPS | DGPS |
|--------------|-----|------|
| Multipath | 0.6 | 0.6 |
| Ephemeris | 2.5 | 0 |
| Troposphere | 0.5 | 0.2 |
| Ionosphere | 5.0 | 0.4 |

DGPS measurement errors (x , y , z) in the order of 15 m and beyond are not unusual in some applications. In order to improve the measurement accuracy, postprocessing of the raw measurement data using appropriate engineering and DSP tools are therefore often inevitable. The accuracy requirement of DGPS data is application, device, and base-rover receiver separation distance dependent. Table 2 shows comparison of a typical GPS and DGPS measurements above the *ellipsoid* (vertical position, similar to mean sea level, a grade benchmark) for selected conditions based on field trials of over 3500 s of measurements using a 10 channel GPS instrument. Various DGPS measurements were obtained experimentally using both 12 and 10 channel DGPS receivers at a pre-surveyed position near Tempe, Arizona at an altitude of about 359 m above mean sea level. The readings were taken at the rate of one reading per second. The measurements were taken to illustrate accuracy improvement using DGPS.

Table 2. Statistical analysis of GPS/DGPS measurement of altitude under controlled conditions (Tempe, AZ, 10 channel receiver)

| Parameter | GPS | DGPS |
|-----------|---------|--------|
| σ | 34.55 m | 3.14 m |
| μ | 371.32 | 371.32 |
| Median | 372.53 | 372.11 |
| Mode | 386.00 | 372.11 |

Differentially corrected GPS data can be appropriately transmitted at desired set time interval to reduce processing burden. DGPS readings for 10 distinct elevations (stations), collocated in longitude and latitude were taken to validate known altitudes. The altitude difference between the stations was varied from 0.10 m to 1.0 m for the test site illustrated in Table 2. An average of 1600 (26 min) readings per station were taken. Table 3 shows the statistical data analysis based on raw DGPS measurements and the respective filtered data using a 12 channel DGPS receivers. In these tests, the effect of electric fields near 230 kV overhead lines is tested.

Table 3. Effect of bad data modification, data taken 15 ft directly under 230 kV lines (Tempe, AZ, approximate electric field strength 0.290 kV/cm, 12 channel receiver)

| DGPS sample parameters | | | | Statistical parameter for DGPS measurements | | |
|------------------------|---------|----------|---------|---|----------------|---------------|
| Data type | Station | Size n | z (m) | \bar{z} (m) | σ_z (m) | 90 % CI (m) |
| Filtered | 3 | 1696 | 359.7 | 359.4 | 0.3 | 359.46-359.48 |
| | 4 | 1654 | 359.7 | 359.43 | 0.3 | 359.42-359.45 |
| | 6 | 997 | 360.5 | 360.39 | 0.3 | 360.38-360.41 |
| | 9 | 1780 | 359.7 | 359.93 | 0.2 | 359.92-359.94 |
| | 10 | 1310 | 359.5 | 359.80 | 0.3 | 359.79-359.82 |
| Raw measurements | 3 | 1696 | 359.7 | 359.30 | 1.8 | 359.40-359.54 |
| | 4 | 1654 | 359.7 | 359.47 | 1.8 | 359.36-359.51 |
| | 6 | 997 | 360.5 | 360.77 | 1.3 | 360.33-360.46 |
| | 9 | 1780 | 359.7 | 359.83 | 1.2 | 359.88-359.98 |
| | 10 | 1310 | 359.5 | 359.85 | 1.5 | 359.74-359.87 |

The confidence interval, (CI) is defined as,

$$CI = \bar{z} \pm \beta(\sigma_z / \sqrt{n}) \quad (2)$$

where, \bar{z} is the mean of n number of samples of raw or filtered data and σ_z is the respective standard deviation. The constant coefficient β is dependent on the probability for which the sample mean lies within the confidence interval (e. g., $\beta=1.9600$ for CI=95 %). Note that σ_z in Table 3 is improved (reduced) in the case of statistical

analysis using the filtered data compared to that of the raw data. Consequently, the confidence interval is narrowed respectively as shown in Table 3.

The main digital processing techniques considered are shown in Fig. 1. Illustrated are bad data identification and rejection (based on a σ -calculation and $\pm 1\sigma$ rejection), and three estimating procedures: moving window time averaging, least squares state estimation, and wavelet spectrum calculation and analysis. Various combinations of these methods are illustrated in Fig. 1. Even though options 1 and 3 in Fig. 1 yield better results compared with that of the raw DGPS data, their performance were not closer to that of options 2 and 4. The results of LSPE and Haar wavelet transform analysis (options 2 and 4) are presented in this paper. These are found to be most applicable for the DSP of DGPS vertical positioning data in a 60 Hz electric field.

III. Least squares parameter estimation

The concept of weighted LSPE is an old one. The method applied here is based on the utilization of measurements, z of the vertical position taken from the physical process to obtain parameter vector x . Denoting the estimate of x as \hat{x} , the weighted LSPE algorithm is

$$z = Hx \quad (3)$$

$$\hat{x} = (\sqrt{W}H)^+ \sqrt{W}z \quad (4)$$

where $(\bullet)^+$ denotes the Moore-Penrose pseudoinverse of a matrix [5, 20]. The matrix W is a weighting factor selected to maximize the utilization of most accurate measurement data. The measurement residual $J(x)$ is described by,

$$\min_x J(x) = \sum_{i=1}^{N_m} \frac{[z_i - (x)]^2}{\sigma_i^2} \quad (5)$$

where, z_i is the i^{th} measured quantity, x is the true value being measured by the i^{th} measurement, σ_i^2 is the variance for the i^{th} measurement, with N_m being the number of sample measurements.

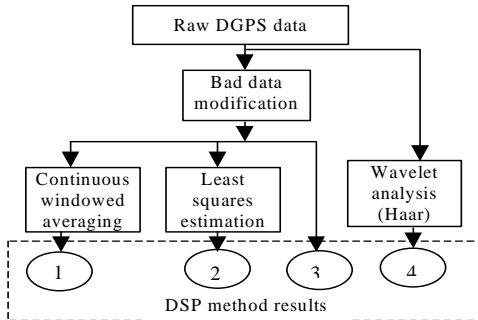


Fig. 1 Selected digital signal processing methods

In this application, vector z is the measured altitudes using DGPS and x are the true altitude positions of the remote GPS receiver. In trying to capture the nonlinear behavior of the error, the LSPE method adopted is formulated as,

$$\hat{z}(n) = Ax(n) + By(n) + Cz(n) + Dx^2(n) + Ey^2(n) + Fz^2(n) \quad (6)$$

where $x(n)$, $y(n)$, $z(n)$ are the sampled readings at certain time that produce the corresponding vertical measurement estimation $\hat{z}(n)$. Using the set of measurements $x(n)$, $y(n)$, $z(n)$ taken for a set of known (i. e., controlled) altitude z_o and replacing $\hat{z}(n)$ with z_o the above equation can be expressed in matrix form as follows,

$$Z_{known} = X\Theta \quad (7)$$

where $\Theta = [A \ B \ C \ D \ E \ F]^T$ are determined using the measurements corresponding to a known z_o . Thus, the parameters $[A, B, C, D, E, F]$ are computed using simple state estimation concept. One formulation involves the Moore-Penrose pseudoinverse of the matrix X .

IV. Wavelet analysis of DGPS data

A wavelet may be described as a waveform of effectively limited duration that has an average value of zero but nonzero integral of the square. Unlike Fourier analysis, which consists of breaking up a signal into sine waves of various frequency components, the wavelet analysis decomposes a signal into shifted and scaled versions of the mother wavelet. This produces a time-scaled view of a signal. Wavelet analysis provides an alternative method for decomposing and reconstructing a given signal $f(t)$, into its constituent parts. Hence, it can provide information about signal patterns and behavior, or capture the location of local oscillations that represents a particular feature at a specific frequency level. Thus, the technique is capable of revealing data trends and discontinuities.

There is a volume of literature on the subject of wavelet transforms and their applications. Some selected few are given in [12-17]. The dilation and translation features of a wavelet transform can be described by a set of functions of the form,

$$\psi_{ab}(x) = |a|^{-1/2} \psi\left(\frac{x-b}{a}\right). \quad (8)$$

representing a set of functions formed by dilations, that are controlled by a positive real number $a \in R^+$ and translations that are controlled by the real number $b \in R$, of a single function $\psi(x)$, which is also known as the mother wavelet. The mother wavelet appears as a local oscillation. In Equation (8), the dilation parameter a controls the width and rate of the local oscillation and hence, can be thought of intuitively as controlling the frequency of $\psi_{ab}(x)$. The translation parameter, b moves the wavelets throughout the domain. The continuous wavelet transform (CWT) of a signal $f(t)$ is described in Equation (9) as an integral of the signal multiplied by a scaled, shifted version of the wavelet function ψ ,

$$C_w(\text{scale}, \text{position}) = \int_{-\infty}^{\infty} f(t)\psi(\text{scale}, \text{position}, t)dt \quad (9)$$

The result of the CWT are many wavelet coefficients C_w . These coefficients are functions of scale and position. The constituent wavelets of the original signal can be regenerated by summing the product of each coefficient and appropriately scaled and shifted wavelet. The identity of most signals, can be traced to a low-frequency content (approximation) of the measurement. The high-frequency content (detail), on the other hand, imparts flavor [14]. In wavelet analysis, the approximation A as shown in the basic filtering process illustrated in Fig. 2 is the high-scale, low-frequency (i.e. identity) components of the given signal. The details D are the low-scale, high frequency (flavor or nuance) components.

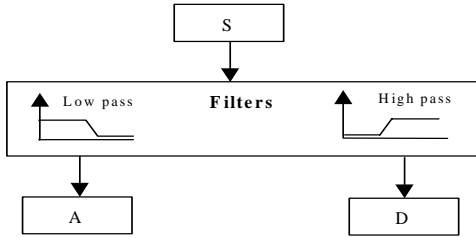


Fig. 2 Basic level of wavelet transform filtering process

In Fig. 2, the original signal passes through two complementary filters and emerges as two signals. The scaling function is similar to the wavelet function and, can be determined by the low pass filters. Therefore, it is associated with the approximation ‘A’ of the wavelet decomposition. In this paper, the approximation component of the DGPS signal is used for data analysis.

Wavelets have been applied in a variety of engineering and science applications in which measurement accuracy is to be improved. In this paper, the application area is DGPS technology for overhead conductor sag measurement. The distinctive nature of the data under analysis calls for the use of the Haar wavelet transform as a postprocessing technique to enhance the accuracy of the raw DGPS measurement data. Wavelet transforms can be used to compress or de-noise a signal without appreciable degradation hence, unlike the LSPE method, the use of the Haar wavelets for data analysis does not require pre-identification and modification of bad data from the raw (original) DGPS signal.

Fig. 3 shows the decomposition of the raw DGPS measurement data, s using the Haar wavelet. The signal (data) represents wavelet components of twelve sub-signal levels for the ten different measured stations. In this case, a level eleven ($n=11$) Haar [14] wavelet is used. For the original DGPS data (signal), s consisting of about 18,555 data points (i.e. $N=2^n \cong 2^{14}$) and sampled at a rate of one measurement per second, there will be about fifteen ($n+1=15$) wavelet levels available.

It can be seen from Fig. 3 that the trend of the quantitative values of altitudes above ellipsoid in meters of the approximation component, $a11$ matches that of the original signal, s to a significant extent. It is to be noted that the shape of the decomposed signal components depends on the shapes of the analyzing wavelet which in turn determine the shape of the building blocks from which a particular signal is constructed.

Decomposed DGPS
Altitude (m)

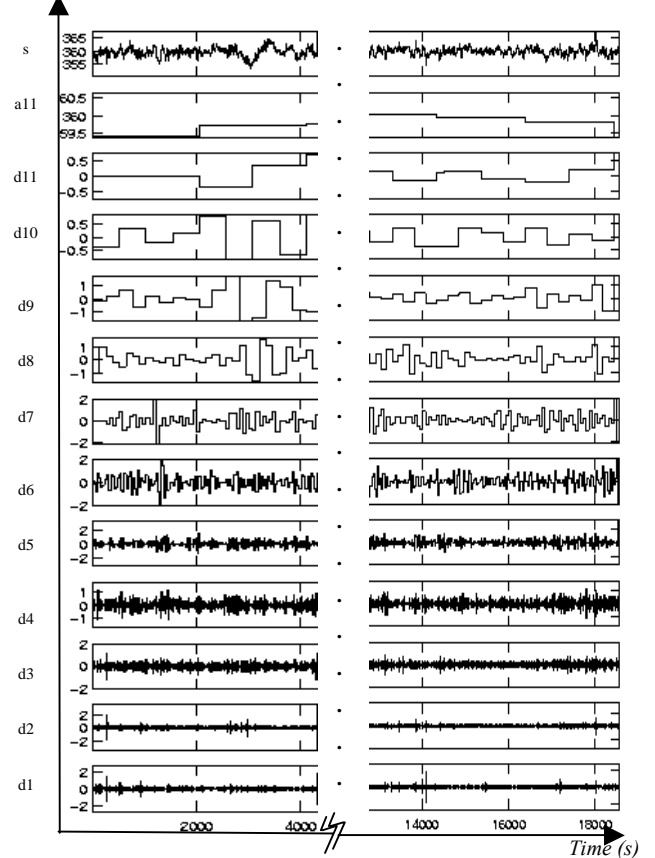


Fig. 3 Decomposed DGPS vertical position signal using Haar wavelets

Recall that wavelet decomposition of a signal has two main elements: the approximated and the detailed. In Fig. 3, the approximation level is shown as $a11$ with its associated detailed components as $d1$ through $d11$. The sum of the various levels results in a signal $s(t)$ at the top of the Fig. 3. References [13, 14] show how to obtain the approximated and detailed components. For practical purposes, the wavelets toolbox of MATLAB software is used to generate these individual components for the given 10 station DGPS measurement data.

V. Quantification of Error

For the purpose of comparing the error resulting from Haar wavelet transforms and the previously

assessed LSPE method, the approximation component (i.e. a_{11}) of the decomposed DGPS signal has been extracted. Fig. 4 shows the estimated altitude above ellipsoid resulting from the extracted Haar wavelet transform level 11 approximation (i. e., a_{11}) of the decomposed signal and the actual (i. e., controlled) altitude above ellipsoid. As can be seen from Fig. 4, the resulting altitude from a_{11} closely matches that of the actual or controlled altitudes above ellipsoid.

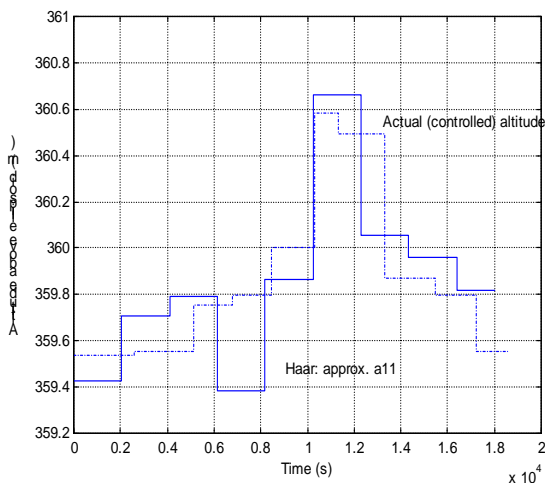


Fig. 4 Comparison of actual altitude measurements with reconstructed Haar approximation, a_{11}

The respective errors or deviations in the LSPE (i. e., error in LSPE) and that of the a_{11} methods from the actual altitudes are depicted in Fig. 5. For the DGPS altitude data being studied, the wavelet approach (a_{11}) tends to have relatively better performance than the LSPE in most cases as shown in Fig. 5.

The confidence index resulting from the two selected methods, a_{11} and LSPE are shown in Figures 6 and 7. These data are for DGPS measurements taken in the vicinity of 230 kV overhead transmission circuits for a 12 channel receiver. It can be seen that for a 70% confidence level the Haar wavelet approximation presents lower error of about 17.2 cm as opposed to 21.5 cm for the LSPE. Due to the so-called end effect phenomenon in wavelet transform analysis, the accuracy of the approximated component is distorted. With appropriate curve fitting techniques it can be seen that the Haar wavelet used in this analysis outperforms the LSPE method. A detailed analysis resulting from the use of bad data identification and modification, artificial neural network estimation (ANNE) and LSPE methods are given in [1, 18]. A brief summary of the resulting accuracy for selected confidence levels is given in Table 4.

An accurate real time overhead conductor position (x, y, z, t) information can be used to redistribute power flow, detect the extent of conductor movement in the x-y plane in a remote location. Equally important is the use of overhead conductor sag information for dy-

namic thermal line ratings [1, 18] and phase measurement applications.

Corona [19] discharge is a potential source of interference in communication systems in the close proximity of high voltage environment. Field trial testing conducted in a laboratory environment and at the Ocotillo substation in Tempe, Arizona indicates the feasibility of the DGPS signal reception for measurements taken at about 14 ft directly below 230 kV lines. However, the severe existence of such a phenomenon (i. e., corona) may affect the normal operation of the DGPS based conductor sag measurement instrument together with the communication links being used for data transfers. The effect of corona on DGPS measurement in the vicinity of discharges needs further investigation that is beyond the scope of this paper; however, no rover - base radio communication problems were observed for 900 MHz technology.

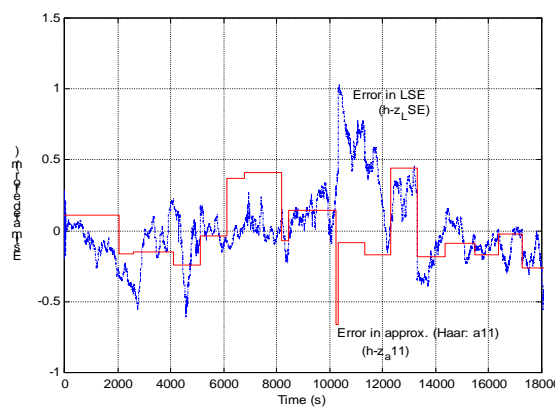


Fig. 5 LSPE vs. Haar wavelet errors

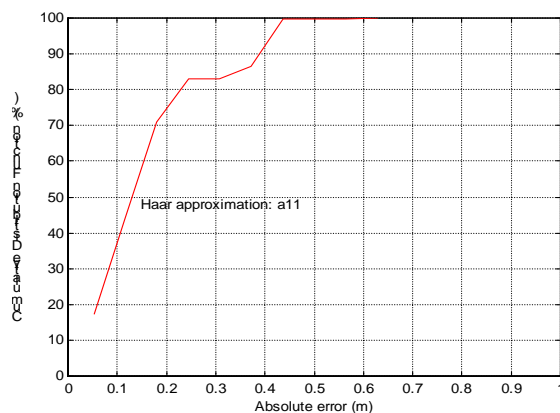


Fig. 6 Cumulative error in altitude (z) measurements for Haar wavelet (a_{11})

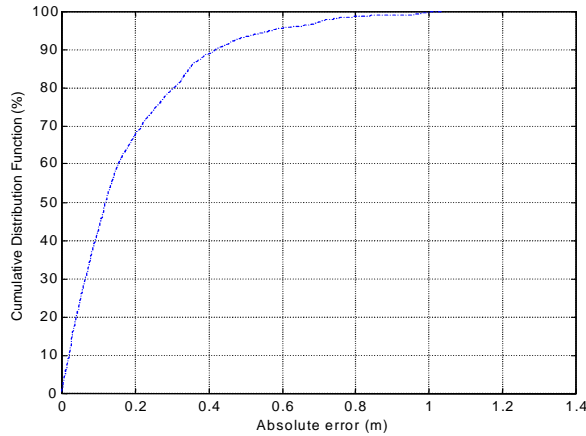


Fig. 7. Cumulative error in altitude (z) measurements for LSPE analysis

Table 4 Selected confidence levels of DGPS altitude measurement near 230 kV transmission lines

| Confidence Index (%) | Absolute error (cm) | | |
|----------------------|------------------------------------|------|------|
| | Haar wavelet (approx. <i>all</i>) | ANNE | LSPE |
| 90 | 30.0* | 37.4 | 41.9 |
| 70 | 17.2 | 19.6 | 21.5 |
| 60 | 15.4 | 14.6 | 15.4 |

*Approximate interpolated value

VI. Conclusions

The power engineering applications of GPS technologies, especially those that relate to the measurement of vertical position have been discussed. A DGPS based conductor sag instrument has been prototyped and used to measure altitudes.

The LSPE method in combination with bad data identification and correction, and Haar wavelet transforms have been utilized to reduce the error of raw DGPS measurements. One of the main advantages of the wavelet approach is that it does not require initial bad data identification and modification, a cumbersome filtering process needed for the LSPE method. The results show that both the LSPE and Haar wavelet approaches exhibit competitive results and reduce the error significantly. The DGPS measurement data accuracy enhancement using the Haar wavelet transform analysis can be considered as a better method. A typical error at the 60 % confidence level is 15.4 cm in the DGPS measurements.

Acknowledgements

The authors acknowledge Arizona Public Service and Entergy in New Orleans whose sponsorships were critical to the research project. The work was done under the auspices of the National Science Foundation Power Systems Engineering Research Center (PSERC).

References

[1] C. Mensah-Bonsu, U. Fernández Krekeler, G. T. Heydt, Y. Hover-son, J. Schilleci; B. Agrawal, "Application of the Global Positioning System to the Measurement of Overhead Power Transmission Conduc-

tor sag," Submitted for publication, IEEE Transactions on Power Delivery, 1999.

[2] U. Fernández, C. Mensah-Bonsu, J. Wells, G. Heydt, "Calculation of the Maximum Steady State Transmission Capacity of a System," Proceedings of the 30th North American Power Symposium, Cleveland, Ohio, October 19-20, 1998, pp. 300-305.

[3] J. Hurn, Differential GPS Explained, Trimble Navigation Ltd., Sunnyvale, CA 1993.

[4] E. Kaplan, Understanding GPS: Principles and Applications, Artech House Telecommunications Library, 1996.

[5] G. T. Heydt, Computer Analysis Methods for Power Systems, Stars in a Circle Publications, Scottsdale, Arizona, 1998.

[6] P. Crossley, "Future of the Global Positioning System In Power Systems," Developments in the Use of Global Positioning Systems, 1994, pp. 7/1-7/5.

[7] G. Harkleroad, W. Tang, N. Johnson, "Estimation of Error Correlation Distance for Differential GPS Operation," Position Location and Navigation Symposium, 1990 Record. The 1990s - A Decade of Excellence in the Navigation Sciences, IEEE PLANS, 1990, pp. 378-382.

[8] T. O. Seppa, "Accurate Ampacity Determination: Temperature Sag Model for Operational Real Time Ratings," IEEE Transactions on Power delivery, Vol. 10, No. 3, July 1995, pp. 1460-1470.

[9] H. Pohlmann, R. Thomas, "Sag Increases Resulting From Conductor Creep on Medium-Voltage Transmission Lines, and the Problem of Measuring Sag on Live Overhead Lines," 12th International Conference on Electricity Distribution, 1993. CIRED, Vol. 3, pp. 3.20/1-5.

[10] D. A. Douglas, A.-A. Edris, "Field Studies of Dynamic Thermal Rating Methods for Overhead Lines," 1999 IEEE Transmission and Distribution Conference, Vol. 2, 1999, pp. 842-851.

[11] W. Z. Black, W. R. Byrd, "Real-Time Ampacity Model for Overhead Lines," IEEE Transactions on Power Apparatus and Systems, vol PAS-102, Vol. 7, July 1983, pp. 2289-2293.

[12] T. H. Koonwinder, Wavelets: An Elementary Treatment of Theory and Applications, World Scientific Publishing, River Edge, NJ, 1993.

[13] D. E. Newland, An Introduction to Random Vibrations, Spectral and Wavelet Analysis, Longman Group UK Limited, Third Edition, 1993.

[14] M. Misiti, Y. Misiti, Oppenheim, G. and Poggi, Jean-Michel Users Guide: Wavelet Toolbox for Use with MATLAB, The Math-Works, Inc., Natick, MA, 1997.

[15] W. A. Wilkinson, M. D. Cox, "Discrete Wavelet Analysis of Power System Transients," IEEE Transactions on Power Systems, Vol. 11, No. 4, November 1996, pp. 2038-2044.

[16] G. T. Heydt, A. W. Galli, "Transient Power Quality Problems Analyzed Using Wavelets," IEEE Transactions on Power Delivery, Vol. 12, No. 2, April 1997, pp. 908-915.

[17] C. K. Chui, An Introduction to Wavelets, Academic Press, New York, 1992.

[18] C. Mensah-Bonsu, Instrumentation and Measurement of Overhead Conductor Sag Using the Differential Global Positioning Satellite System, PhD. thesis, Arizona State University, Tempe, August 2000.

[19] E. Kuffel, W. S. Zaengl, High Voltage Engineering Fundamentals, Pergamon Press, New York, 1984.

[20] J. K. Neter, C. J. Nachtsheim, W Wasserman, Applied Linear Statistical Models, 4th Edition, Times Mirror Higher Education Group, Chicago, 1996.

[21] Anonymous, "Satellite Pictures: Private Eyes in the Sky," The Economist, May 6, 2000, pp. 71 - 73.

Biographies

Chris Mensah-Bonsu holds a Ph.D. degree in Electrical Engineering from Arizona State University. Dr. Mensah-Bonsu has accepted an offer at the California Independent System Operator (CA ISO) as a Market Design Engineer. His interests are in the area of power systems, dynamic

thermal line rating and system reliability issues in the competitive electricity market environment.

Gerald Thomas Heydt holds the Ph.D. degree in Electrical Engineering from Purdue University. He is a member of the National Academy of Engineering. Dr. Heydt is presently a Professor of Electrical Engineering at Arizona State University.